COMPDYN 2015
5th ECCOMAS Thematic Conference on
Computational Methods in Structural Dynamics and Earthquake Engineering
M. Papadrakakis, V. Papadopoulos, V. Plevris (eds.)
Crete Island, Greece, 25–27 May 2015

SEISMIC PERFORMANCE OF HIGH-RISE STEEL MRFs WITH OUTRIGGER AND BELT TRUSSES THROUGH NONLINEAR DYNAMIC FE SIMULATIONS

Emanuele Brunesi[1], Roberto Nascimbene[1], Gian Andrea Rassati[2], Lorenzo Casagrande[3]

[1] EUCENTRE, European Centre for Training and Research in Earthquake Engineering
Via Ferrata 1, 27100 Pavia, Italy
{emanuele.brunesi, roberto.nascimbene}@eucentre.it

[2] Dept. of Civil and Architectural Engineering, University of Cincinnati
765 Baldwin Hall, Cincinnati, OH 45221-0071 USA
Gian.Rassati@uc.edu

[3] EUCENTRE, European Centre for Training and Research in Earthquake Engineering
Via Ferrata 1, 27100 Pavia, Italy
lorenzo.casagrande01@gmail.com

Keywords: high-rise buildings; steel MRFs; outrigger; belt trusses; FE models; nonlinear dynamic analysis.

Abstract. *The work reported herein summarizes the results of a series of nonlinear dynamic FE analyses devoted to assess the main criticalities in the seismic response of high-rise steel MRFs with outrigger and belt trusses. Thirty- and sixty-storey planar frames, extracted from reference three-dimensional structures composed of an internal one-way braced core, are designed in accordance with European rules. The core consists of a CBF system, while outriggers are placed every fifteen stories to limit inter-storey drifts and second order effects. FE models able to account for material and geometric nonlinearities have been developed within an open source FE code, using inelastic force-based fiber elements to model structural members and equivalent nonlinear links to reproduce the behaviour of bolted beam-column joints and welded gusset-plate connections. Out-of-plane imperfections are explicitly included in the braces to allow for potential buckling mechanisms in both braces and gusset plates. NLTHAs have been performed, in comparison with response spectrum analysis, aiming to quantify the potential of such systems, when included in the lateral-force resisting system of modern high-rise steel MRFs. Global and local performance have been investigated in terms of inter-storey drift and acceleration peak profiles and axial force-displacement curves and static-to-seismic load ratios in critical braces at different floor levels. Sensitivity to the structure height has been explored by comparing the response of the two prototype MRFs. Trends are discussed to show that, if accurately designed and detailed, these structural systems provide an optimum combination of stiffness and strength.*

1 INTRODUCTION

Super-tall buildings have become increasingly popular and have large impact on economy and society [1-3]. Such buildings have a complicated structural system consisting of hundreds of different components, including those with complex features and large dimensions. When compared to medium- and low-rise buildings, tall moment resisting frame (MRF) structural systems present several distinctive characteristics in their behavior and peculiar aspects in their design, such as long periods and higher mode effects [1-11]. To ensure safe and economic design, construction and operation under various extreme loading conditions in particular earthquake events, detailed studies are required to predict their response, being the majority of current seismic Standards often unsuitable for them [12-14]. Scaled shaking table tests [15, 16] are at the moment promising analysis techniques for research applications but they are not so easily applicable for design office use. Therefore, high-definition or simplified finite element (FE) idealizations still represent an attractive tool to explore the seismic performance of these complex structural systems, as proposed by a number of research efforts available in literature on that subject [1-11]. If early studies [5-11] introduced simplifications in either FE representation or analysis technique, significant improvements have been more recently achieved [1-4].

In light of this scenario, the present paper details a modeling procedure for large scale nonlinear dynamic simulation of mega-frame systems composed of a concentrically braced frame (CBF) core and belt trusses which are combined to resist vertical and earthquake-induced lateral loads. First, two reference prototypes, the geometric characteristics of which are summarized in the following, have been designed according to current European prescriptions [17], using response spectrum analysis (RSA), and then fiber-based models have been prepared to examine their nonlinear dynamic response using a set of natural ground motions scaled to obtain displacement spectrum compatibility in accordance with EC8 requirements [18, 19].

Hence, global inter-storey drift and acceleration peak profiles, as well as shear and bending moment demands, are collected and their average is compared with the results determined by RSA to highlight design criticalities in current seismic Code provisions [17]. Finally, the local response of these two case-study buildings is discussed in terms of hysteretic behaviour of the braces and peak compressive loads experienced by the outriggers during nonlinear time history analyses (NLTHAs).

2 NONLINEAR DYNAMIC FE ANALYSES

Even though detailed brick- or shell-based FE models, commonly used in seismic analysis of steel and reinforced concrete structural systems and components [20-27], give more insight than equivalent mechanical idealizations, being able to reproduce their local response in terms of stress/strain concentrations, the computational time increases tremendously, requiring necessarily to take advantage of parallel processing on multiprocessor computers. Additionally, a detailed approach is currently almost unfeasible if the response of an entire mega-frame system has to be investigated. By contrast, the complex contribution of bolted [22-25, 28-30] and welded [20, 21, 31, 32] joints can be easily incorporated into classical fiber-based FE models, able to represent the interaction among connection components in an equivalent manner. Thus, mechanical representations have been assumed in this research to include global response and potential failure mechanisms of these systems, as discussed later on. In particular, the prevailing assumptions concerning modeling approach and simulation techniques will be given in the following, after a brief description of the main geometric characteristics and mechanical properties of the thirty- and sixty-storey planar frames examined here. Finally, details of the seismic input selected to perform the series of NLTHAs and RSAs shown in the following section will be provided.

2.1 Description of case-study super-tall buildings

The two prototype thirty- and sixty-storey MRF buildings investigated in this work, namely HR-01 and HR-02, were extracted from reference three-dimensional structures designed for high seismicity (i.e. PGA = 0.40g) in accordance with the current European seismic code [17]. Soil class C (180 m/s < V_s < 360 m/s) was assumed to perform the design by a series of RSAs on three-dimensional models, including vertical seismic component, second order effects and accidental eccentricity of the seismic masses. As depicted in Fig. 1, where a schematic of plan and elevation is provided, the lateral-force resisting system (LFRS) of each high-rise building consisted of an internal one-way CBF core, with outriggers placed every fifteen stories to limit inter-storey drifts and second order effects.

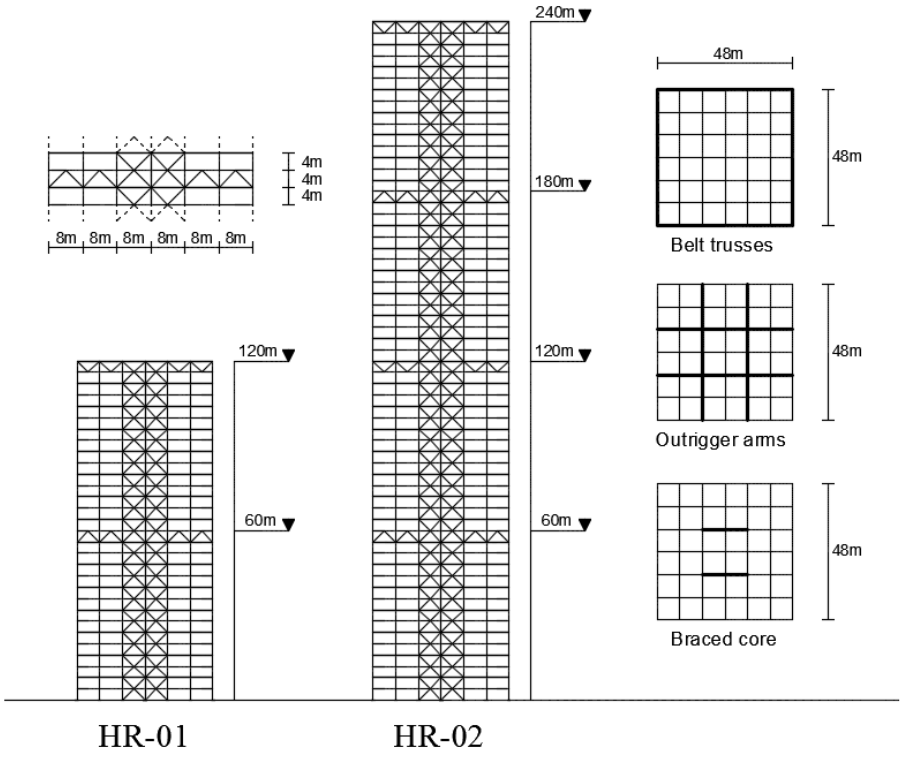

Figure 1: Geometric characteristics of the reference 30- and 60-storey planar frames studied.

The two structural layouts analyzed in this study consisted of a 6x6-bay building; the beam span for all bays was set at 8 m both for transversal and longitudinal direction, while the columns were assumed to have a constant inter-storey height of 4 m, thus implying a total building height of 120 m and 240 m for HR-01 and HR-02, respectively. Dead and live loads were assumed to be 2 kN/m^2 and 4 kN/m^2, respectively. Table 1 summarizes member sizes and mechanical properties adopted for beams, outriggers, columns and braces at different floor levels, while Fig. 2 shows an example of welded gusset-plate and bolted beam-to-column connection systems used to detail the joints of the two structures.

In detail, IPE400 beams were used at all floors for both prototypes, while HD 400x634 and HD 400x1200 tapered profiles were used for the first five columns of HR-01 and HR-02, respectively. Similarly, HD 400x314 profiles were assumed as the outriggers of both structures, while HSS 300x20 and HSS 400x20 braces were chosen in the first five stories for HR-01 and HR-02, respectively. Both brace and column sizes were assumed to decrease along the height of the structure, as presented in Table 1. According to [33], steel grade S-275, S450 and S700 were used for beams, columns and braces, respectively.

	30-storey frames			*60-storey frames*		
	Floor	*Profile*	*Grade*	*Floor*	*Profile*	*Grade*
Columns	1-5	HD 400x634	S450	1-20	HD 400x1200	S450
	6-10	HD 400x509	S450	21-30	HD 400x900	S450
	11-15	HD 400x421	S450	31-40	HD 400x634	S450
	16-20	HD 400x421	S450	41-50	HD 400x509	S450
	21-30	HD 400x237	S450	51-60	HD 400x314	S450
Beams	1-30	IPE400	S275	1-60	IPE400	S275
Outriggers	15/30	HD 400x314	S700	15/30/45/60	HD 400x314	S700
Braces	1-5	HSS 300x20	S700	1-10	HSS 400x20	S700
	6-15	HSS 250x16	S700	11-20	HSS 350x16	S700
	16-20	HSS 200x16	S700	21-30	HSS 300x16	S700
	21-30	HSS 200x16	S700	31-60	HSS 250x16	S700

Table 1: Member sizes and mechanical properties in key structural components for HR-01 and HR-02.

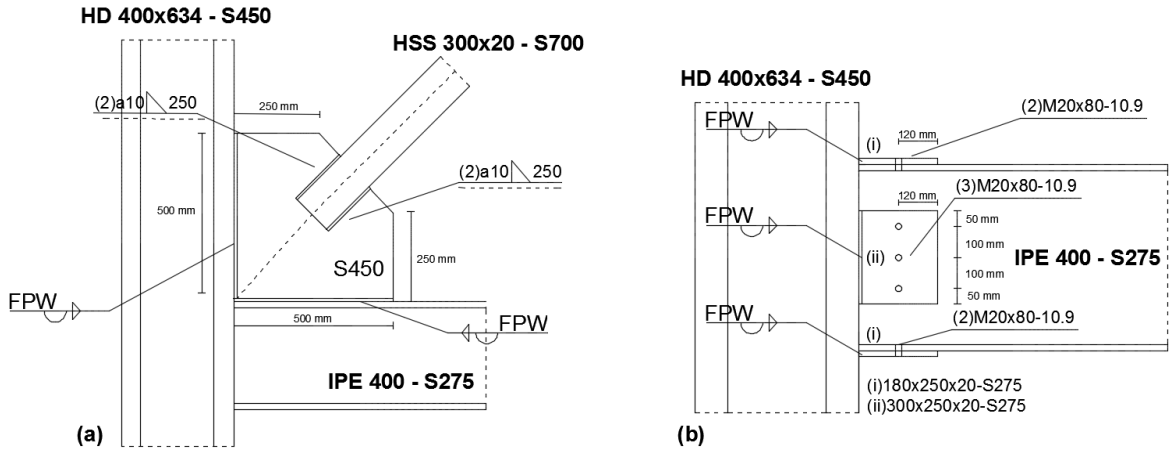

Figure 2: Details of (a) gusset-plate and (b) beam-to-column connections. Note: HR-01 – first floor.

As previously mentioned, Fig. 2 sketches an example of the connection systems used to detail the joints of the two high-rise braced frames. In particular, Fig. 2(a) presents the geometry of the gusset plate used to connect the beam/column and the rectangular hollow section shape brace; fillet welds were provided between the web of the gusset plate and the rectangular HSS brace, while full penetration welds (FPW) were chosen to connect the edge of the gusset plate and the flanges of beam and column. In addition, Fig. 2(b) shows the layout of a bolted beam-to-column connection used in the first floor of HR-01. Three M20x80 – 10.9 bolts were used to bolt the shear tab to the web of the beam and two M20x80 – 10.9 bolts were provided between a 180x250x20 mm plate, welded by FPW to the flange of the column, and the flange of the beam, in accordance with the prescriptions of [34].

2.2 Modeling approach and seismic input

To investigate the seismic response of these two case-study buildings, a series of NLTHAs were carried out, using the open source platform OpenSees [35] to construct their fiber-based idealizations able to account for material and geometrical nonlinearities through classical con-

stitutive law and co-rotational transformation [36]. As suggested in [36], inelastic force-based fiber elements, with five integration points, were used to model structural members, assuming a bi-linear stress-strain relationship with isotropic strain hardening to reproduce the permanent deformations exhibited by plastic materials during the loading-unloading history. The tangent stiffness-proportional Rayleigh damping calibrated on the first period of the two mega-frames was employed to perform the series of nonlinear dynamic analyses, as done in [37, 36]. Finally, the Krylov subspace algorithm was used to iteratively equilibrate loads, since it has a larger radius of convergence and requires fewer matrix factorizations than Newton-Raphson [38, 36].

Fig. 3 shows a schematic of the modeling approach used for brace and gusset-plate connections [20, 21, 31, 32]. The model consists of two inelastic force-based beam-column elements, each of which having five integration points and a discretized fiber section. In order to capture the effects of gusset end restraint [20, 21, 31, 32], the present paper takes advantage of an additional inelastic force-based beam-column element of length $2t$ – where t is the thickness of the gusset plate – at each end of the brace. A set of rigid elements is included to represent the confined portions of beam, column and gusset plate, as shown by [20, 21, 31, 32]. To account for potential buckling mechanisms in both braces and gusset plates, an out-of-plane imperfection equal to 0.1% of the entire brace length is applied, while the nodes of both beam and columns are constrained to deform in-plane only. Similarly, an equivalent idealization developed along the lines of classical mechanical/component approach [22-25] is used to incorporate the cyclic behaviour of bolted joints.

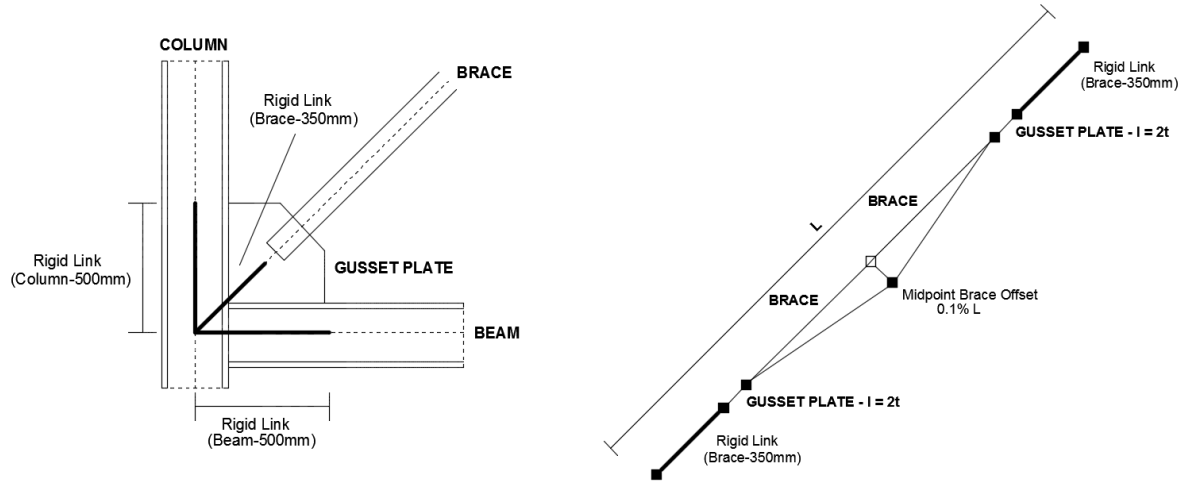

Figure 3: Schematic of the modeling approach used for gusset-plate connections.

A classical displacement/rotation-based convergence criterion, with a threshold set equal to 10^{-3} was adopted for the series of NLTHAs performed by assuming an auto-update integration time-step of the order of one-tenth of the time sampling of the ground motions considered [18, 19]. In particular, a set of ten natural records scaled to obtain displacement spectrum compatibility according to EC8 requirements [17] was selected herein; type 1 spectrum with a PGA of 0.4g and soil type C with T_D equal to 8s were the prevailing criteria for this suite. Further and more comprehensive information may be found in [18, 19].

3 RESULTS AND DISCUSSION

In the following discussion, the main results obtained from the series of numerical analyses carried out (i.e. RSAs and NLTHAs) will be summarized. In particular, the responses of these

two high-rise mega-frame structures will be compared and used to describe the global and local behaviour of their LFRSs, when subjected to severe earthquake-induced demands. A general overview of their main characteristics is given herein, and specific aspects are referenced when needed to explain key points. Particular care is paid to the response of braces and joints, showing their influence on the global structural performance.

3.1 Global performance of mega-frame systems

The global responses of the two super-tall buildings studied are provided in Fig. 4, in terms of inter-storey drift and acceleration peak profiles from NLTHAs and RSAs. In addition, peak displacements obtained at each floor are collected in Fig. 5 for both structures.

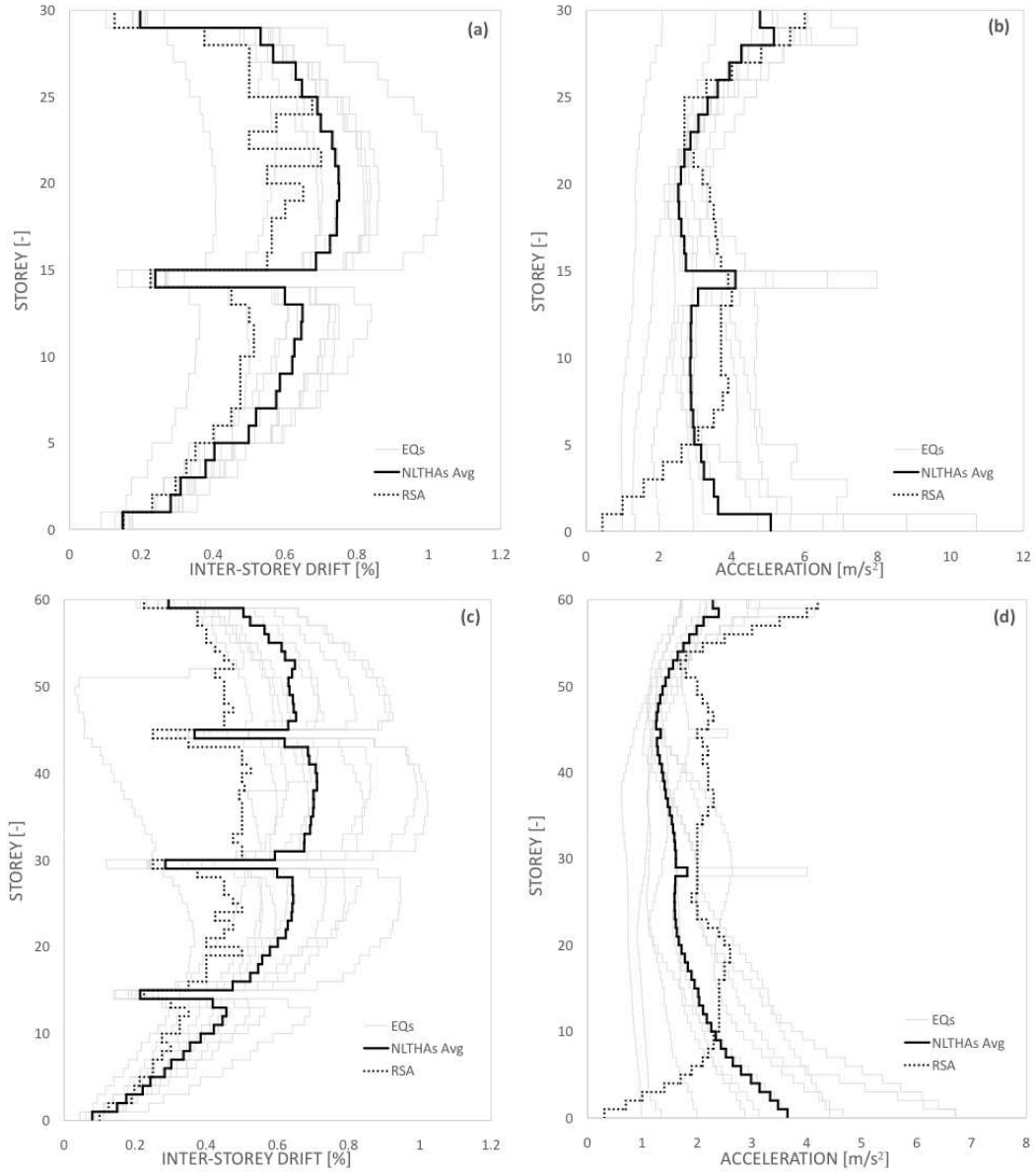

Figure 4: Inter-storey drift and acceleration peak profiles in HR-01 and HR-02 from NLTHAs and RSAs.

Peak roof displacements of up to 0.77 m and 1.83 m were observed for HR-01 and HR-02, in the case of the most severe record, while values of about 0.61 m and 1.17 m were computed in average, thus showing peaks 20% and 36% lower for HR-01 and HR-02, respectively. RSA

deviates from the average of the ten NLTHAs at approximately mid-height, reaching a discrepancy of about 10% and 20% at the top storey of the thirty- and sixty-storey buildings. A fairly cantilevered shape, with discontinuities in correspondence to the outriggers, were predicted for both structures. This trend is even more visible in terms of inter-storey drifts and accelerations, as shown in Fig. 4. In detail, peak inter-storey drifts of approximately 0.75% and 1.00% were shown to occur at two-thirds of the total structural height for both HR-01 and HR-02, in average and in case of the worst event, respectively. The stiffening effect provided by the outriggers was proven to be significant for both structural systems, as evidenced by a pronounced reduction in terms of peak inter-storey drifts experienced by dynamic simulations. By contrast, these members caused a significant acceleration and shear force demand in correspondence to them, as discussed later on.

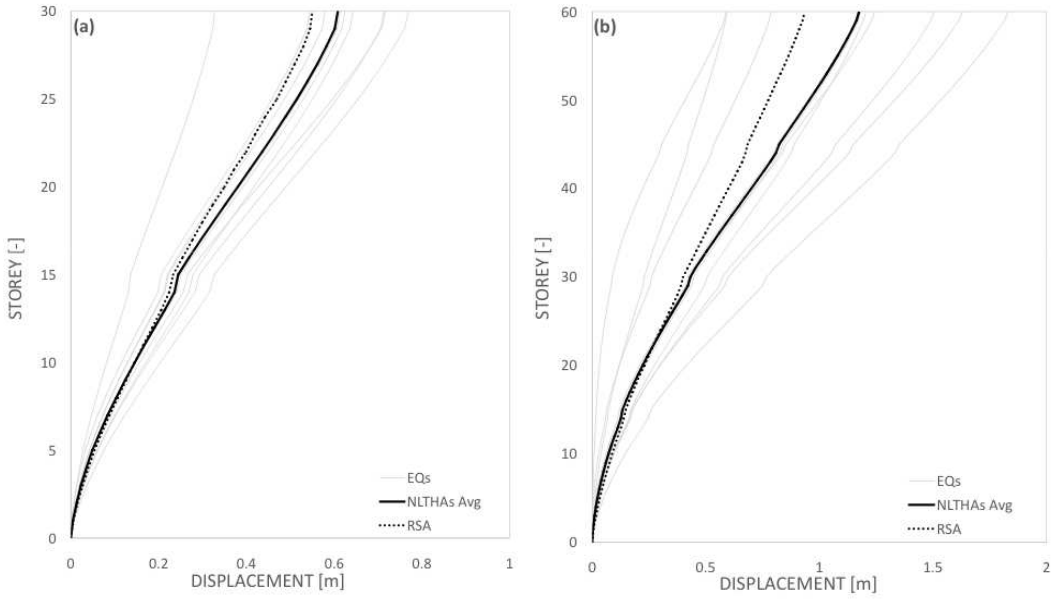

Figure 5: Peak displacement profiles for (a) HR-01 and (b) HR-02.

This trend is particularly evident for the stiffest of the two structures – HR-01 – which has a fundamental period more than halved in comparison with HR-02 (i.e. 2.73 s vs. 6.17 s). The peaks in terms of floor acceleration were approximately 0.53g and 0.37g in HR-01 and HR-02, respectively. If the most severe ground motion is taken as reference, peaks of up to 1.09g and 0.68g were undergone during NLTHAs. Finally, the higher modes contribution is pronounced, particularly in the upper stories of the tallest building, as a consequence of a higher flexibility.

Hence, the series of nonlinear dynamic simulations conducted have confirmed that, if accurately designed, these structural systems provide an optimum combination of overall stiffness and strength for super-tall mega-framed buildings, inducing a good balance between drift and acceleration demands.

3.2 Local response of key structural components

Once the global responses of the two high-rise structures were quantified, the local performance of key components, such as columns, braces and outriggers, will be discussed in detail. Axial load, bending moment and shear force peak profiles in different columns will be shown, as well as the hysteretic response of critical braces in terms of axial force-displacement curves. In addition, the peak profiles of the static-to-seismic axial load ratios will be computed in two reference columns for both structures.

To evidence the effects caused by the in-plane rotation of the outriggers, Fig. 6 collects the set of earthquake-induced compressive loads experienced by the leftmost and central columns of HR-01 and HR-02 in comparison with those obtained in static conditions (i.e. dead and live loads in seismic combination).

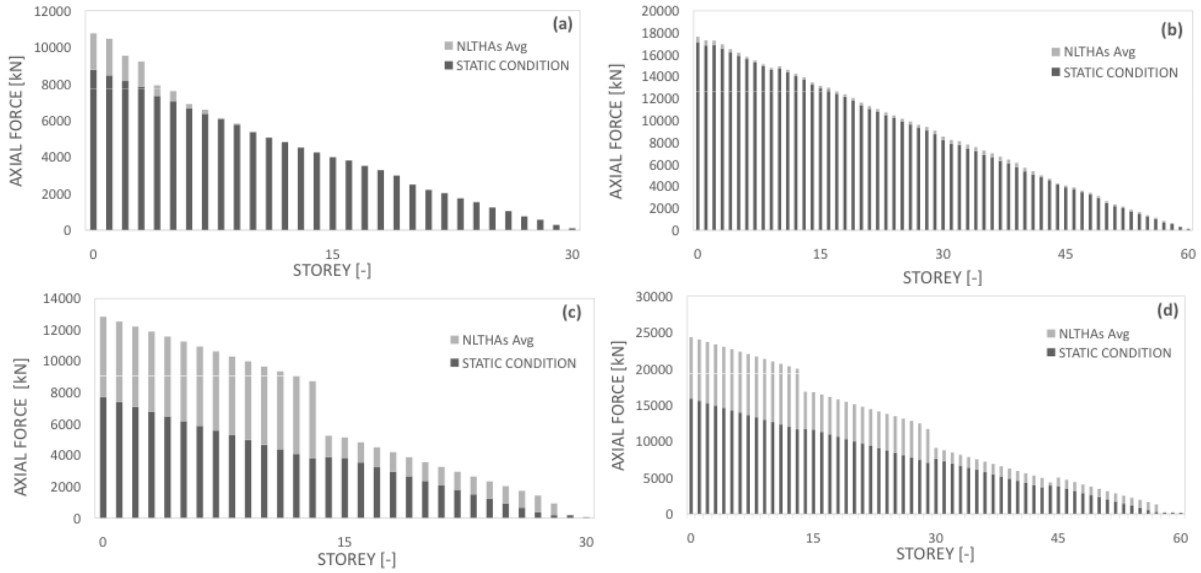

Figure 6: Peak profiles of static-to-seismic axial load ratios in the central column of (a) HR-01 and (b) HR-02 and in the leftmost column of (c) HR01 and (d) HR02, respectively.

As expected, the central column of both building are shown to remain almost unaffected by the dynamic excitation, since negligibly small extra-loads were observed, particularly for HR-02. By contrast, the contribution to lateral resistance ensured by the outriggers caused significant compressive overloads to be transferred to the lateral columns. In detail, an approximately 40% and 30% increase was computed at the base of HR-01 and HR-02, respectively; as the height of the structure increases, this effect tends to decrease, approximately showing a linear piecewise slope with the structure height. Pronounced discontinuities were again predicted in correspondence to the outriggers.

Therefore, only the results collected for the leftmost column of both structures will be presented hereafter. In particular, the bending moment and shear force peak profiles predicted by NLTHAs and RSA for HR-01 and HR-02 are shown in Fig. 7 and Fig. 8. High concentrations are again obtained in correspondence to the outriggers, as a consequence of those highlighted in terms of floor acceleration (see Fig. 4). As previously mentioned, RSA tends to visibly underestimate bending moment and shear force demands from NLTHAs. In some cases, values more than halved were determined.

An example of the axial force-displacement capacity curves predicted in a brace at the first floor is presented, in Fig. 9, to characterize the hysteretic behaviour of such a critical member. A pseudoelastic cyclic response governed by strength rather than ductility can be observed for both HR-01 and HR-02. The narrow hysteresis loops were shown to be too unstable to develop a well-established dissipative mechanism. Compressive peak forces of up to 5000 kN and 7000 kN were obtained, in this case, for the thirty- and sixty-storey CBF structure, respectively. As shown in Fig. 10, where the compressive force peak profiles constructed for HR-01 and HR-02 are provided, a similar demand was predicted in average in the upper stories where the outriggers are placed. RSA is confirmed to underestimate NLTHAs, particularly in the bottom and intermediate floor levels.

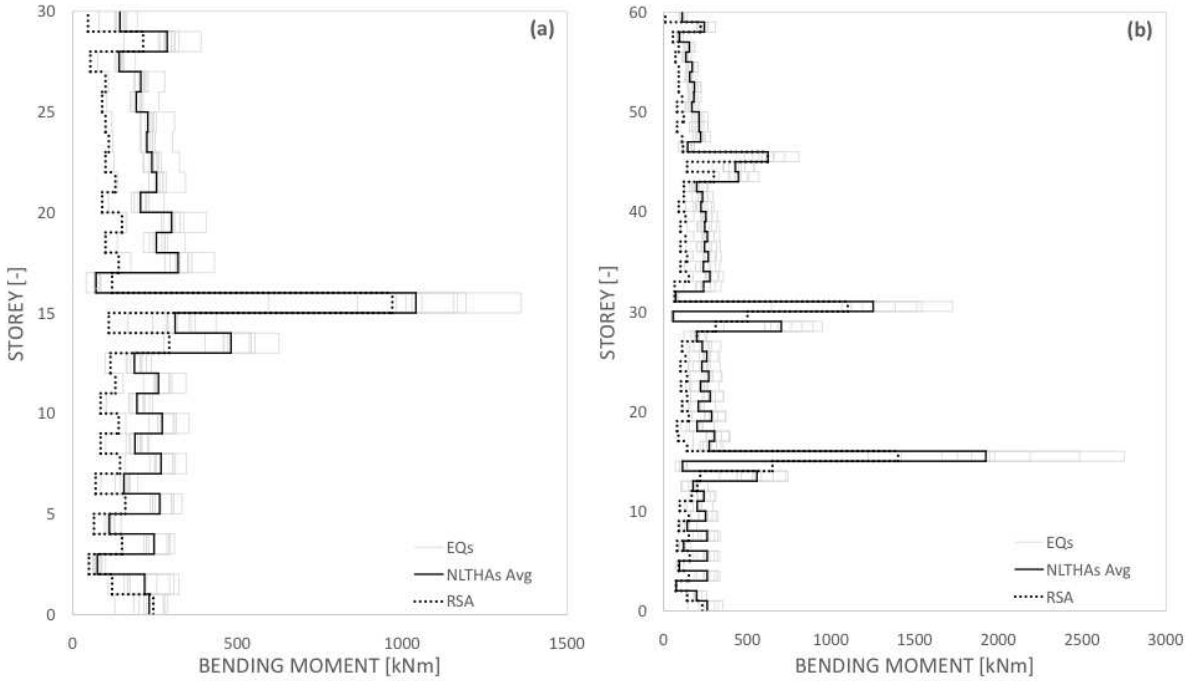

Figure 7: Bending moment peak profiles in the leftmost column of (a) HR-01 and (b) HR-02, respectively.

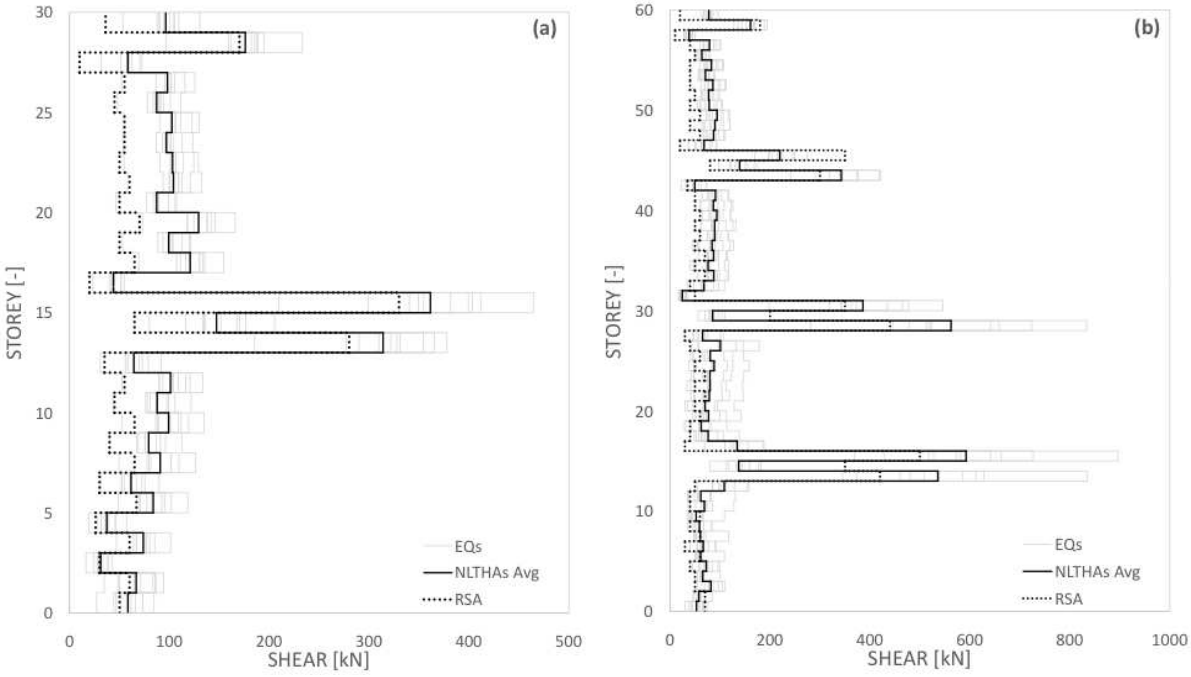

Figure 8: Shear force peak profiles in the leftmost column of (a) HR-01 and (b) HR-02, respectively.

In detail, a discrepancy of about 40% was predicted for both structures, if RSA and the average from NLTHAs are compared.

In Fig. 11, a comparison is provided between the compressive peak loads determined under seismic excitation and static conditions, in the most critical brace, for both high-rise buildings. Dynamic effects much more pronounced than those evidenced in the columns can be observed. Furthermore, Fig. 12 collects the series of NLTHA-to-RSA axial force ratios (R) computed in leftmost and rightmost braces of the core.

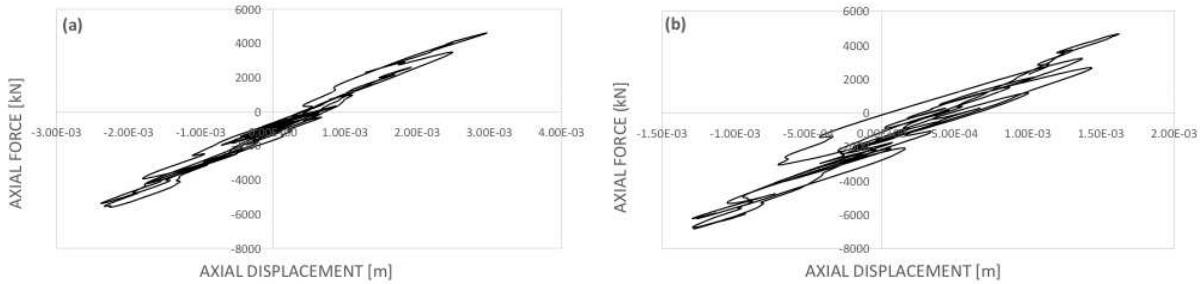

Figure 9: Hysteretic behaviour of a critical brace at the first floor for (a) HR-01 and (b) HR-02.

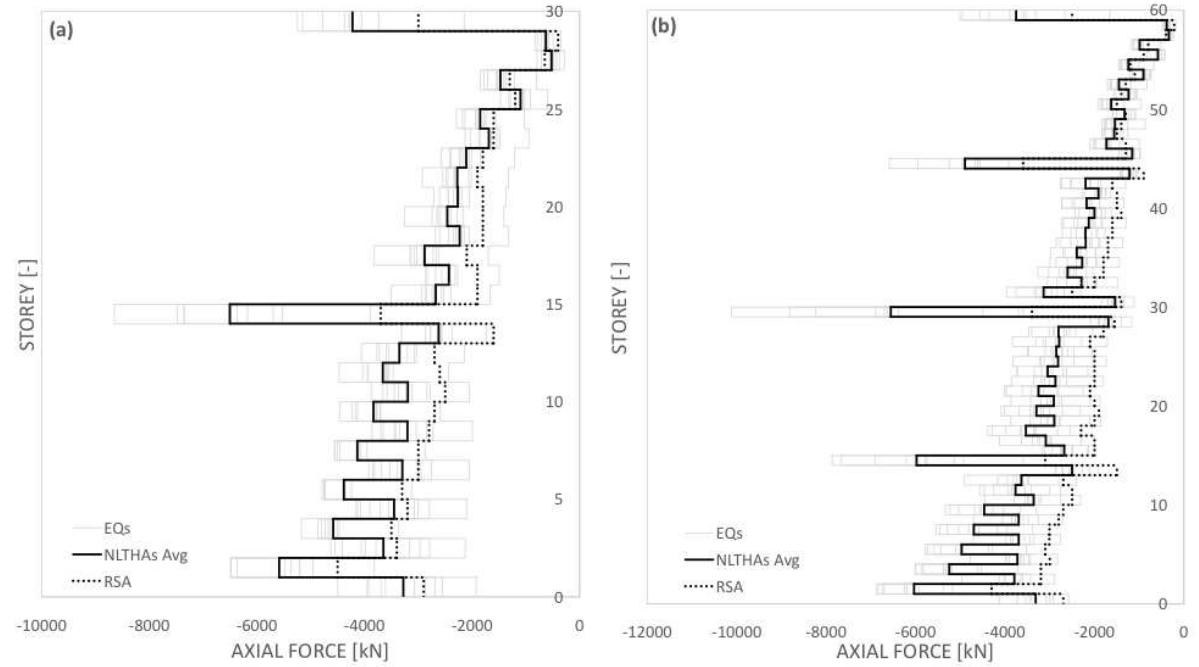

Figure 10: Compressive force peak profiles in a critical brace of the core for (a) HR-01 and (b) HR-02.

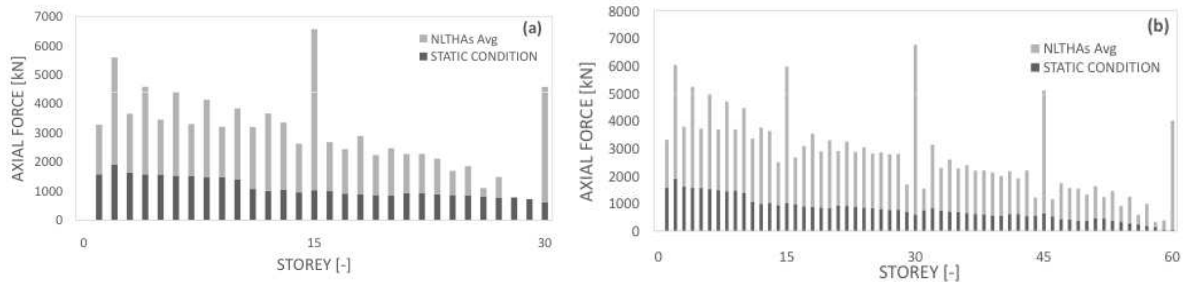

Figure 11: Static-to-seismic axial load ratios in a critical brace of (a) HR-01 and (b) HR-02, respectively.

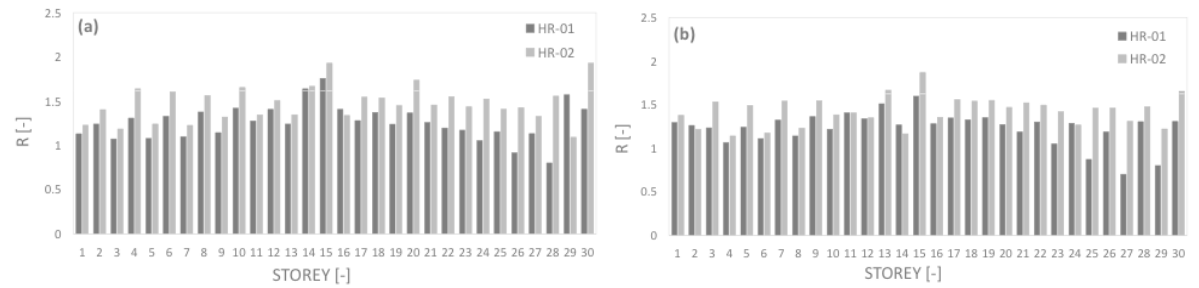

Figure 12: NLTHA-to-RSA axial load ratios in the (a) leftmost and (b) rightmost brace of the core.

Being the mismatch between RSA and NLTHAs in the braces higher than that observed in other members, particular care has to be paid to the earthquake-induced demand considered to design the related joints. In particular, EC8 recommends the following equation to be used for this purpose:

$$R_d = 1.1 \gamma_{ov} R_{fy} \tag{1}$$

where R_d is the axial resistance of the connection, γ_{ov} is the material overstrength factor and R_{fy} is the plastic resistance of the connected dissipative member.

Fig. 13 provides a comparison between the axial force peak profiles obtained by this EC8-based approach and the average from NLTHAs, showing the former to lead to unconservative demands, particularly in correspondence to the outriggers.

Finally, Fig. 14 presents a comparison between the peak axial forces predicted by RSA and NLTHAs in the outriggers placed at the 30th storey of both structures.

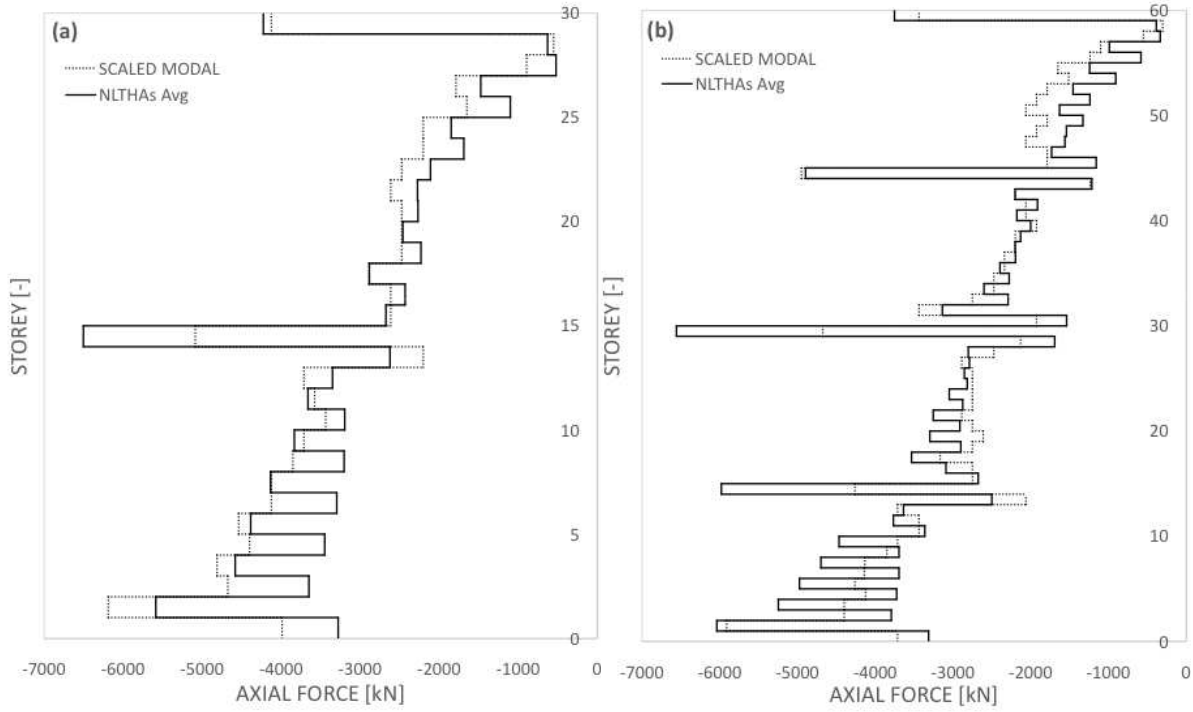

Figure 13: NLTHAs vs. EC8-based demand – axial load peak profiles in a brace of (a) HR01 and (b) HR-02.

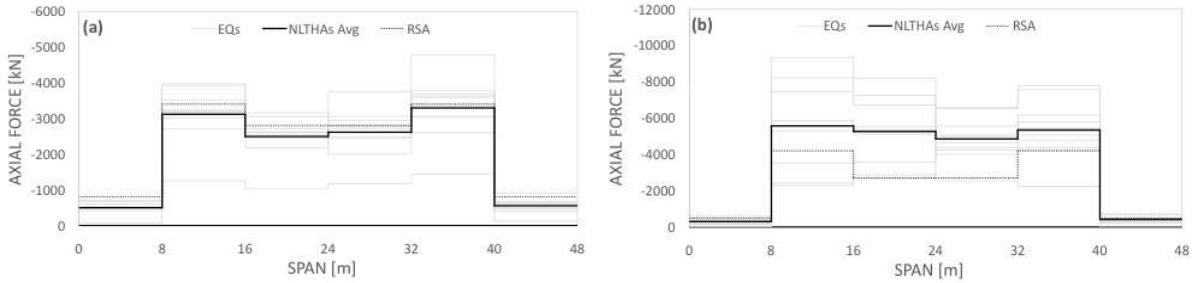

Figure 14: Axial forces in the outriggers at the 30th storey in (a) HR-01 and (b) HR-02, respectively.

Even though a negligibly small differences can be observed between RSA and the average from NLTHAs for HR-01, a larger discrepancy was evidenced in the outriggers at mid-height of the sixty-storey structure.

4 CONCLUSIONS

This paper focuses on the seismic response of super-tall mega-braced frame structures, including outriggers and belt trusses in their LFRS. In detail, thirty- and sixty-storey planar prototype frames, extracted from three-dimensional reference buildings, were designed according to European prescriptions and analyzed, in nonlinear dynamic fashion, to examine both global and local behaviour of structural system and key components. Inelastic force-based fiber elements and mechanical fiber-based idealizations were used to represent structural members and connections in an equivalent manner. NLTHAs were performed in comparison with RSA, using a set of ten natural displacement spectrum compatible records selected from past works as a severe seismic input. The prevailing observations and conclusions drawn from the numerical simulations carried out can be summarized as follows:

- A pseudoelastic response governed by strength rather than ductility was obtained for both structures, thus showing CBFs and outriggers to be effective in limiting inter-storey drifts and second order effects. In particular, peak inter-storey drifts of up to 0.75% and 1.00% were predicted to occur at two-thirds of the total structural height, whether the average of the NLTHAs and the most severe event are considered, respectively.
- Visible discontinuities in displacement, inter-storey drift and floor acceleration peak profiles were shown in correspondence to the outriggers, as a consequence of the significant stiffening effect provided by them, which in turn caused a large increase in bending moment and shear force demands in columns, braces and gusset-plate connections.
- The effects caused by the in-plane rotation of the outriggers were proven to be negligibly small in the central column of both prototypes, while high extra-loads of up to 40% were transferred to the lateral columns. In particular, the compressive force peak profiles were characterized by an approximately linear piecewise decaying slope, with pronounced discontinuities in correspondence to the outriggers.
- RSA tends to largely underestimate NLTHAs and in some cases values more than halved were determined, in terms of local demands on key structural components; a similar consideration can be drawn for peak displacements and inter-storey drifts. Therefore, the use of NLTHAs as a post-design check is reaffirmed to be a crucial aspect for these high-rise systems, the response of which is significantly affected by higher mode effects.
- Sensitivity to the structure height was investigated by comparing the responses of the two prototypes, thus showing current European seismic rules to impose a similar performance point for both HR-01 and HR-02, in terms of global and local behaviour. When accurately designed and detailed, CBFs and outriggers were demonstrated to provide an optimum combination of stiffness and strength for these super-tall buildings, inducing a good balance between drift and acceleration demands.

REFERENCES

[1] H. Fan, Q.S. Li, A.Y. Tuan, L. Xu, Seismic analysis of the world's tallest building. *Journal of Constructional Steel Research*, **65**, 1206-1215, 2009.

[2] X. Lu, X. Lu, H. Guan, W. Zhang, L. Ye, Earthquake-induced collapse simulation of a super-tall mega-braced frame-core tube building. *Journal of Constructional Steel Research*, **82**, 59-71, 2013.

[3] X. Lu, X. Lu, H. Sezen, L. Ye, Development of a simplified model and seismic energy dissipation in a super-tall building. *Engineering Structures*, **67**, 109-122, 2014.

[4] I. Takewaki, S. Murakami, K. Fujita, S. Yoshitomi, M. Tsuji, The 2011 off the Pacific coast of Tohoku earthquake and response of high-rise buildings under long-period ground motions. *Soil Dynamics and Earthquake Engineering*, **31**, 1511-1528, 2011.

[5] M. Poursha, F. Khoshnoudian, A.S. Moghadam, A consecutive modal pushover procedure for estimating the seismic demands of tall buildings. *Engineering Structures*, **31**, 591-599, 2009.

[6] Q.S. Li, Y.H. Zhang, J.R. Wu, J.H. Lin, Seismic random vibration analysis of tall buildings. *Engineering Structures*, **26**, 1767-1778, 2004.

[7] S.A. Meftah, A. Tounsi, A.B. El Abbas, A simplified approach for seismic calculation of a tall building braced by shear walls and thin-walled open section structures. *Engineering Structures*, **29**, 2576-2585, 2007.

[8] J. Ji, A.S. Elnashai, D.A. Kuchma, An analytical framework for seismic fragility analysis of RC high-rise buildings. *Engineering Structures*, **29**, 3197-3209, 2007.

[9] F. Khoshnoudian, M.M.B. Kashani, Assessment of modified consecutive modal pushover analysis for estimating the seismic demands of tall buildings with dual system considering steel concentrically braced frames, *Journal of Constructional Steel Research*, **72**, 155-167, 2012.

[10] M. Poursha, F. Khoshnoudian, A.S. Moghadam, A consecutive modal pushover procedure for nonlinear static analysis of one-way unsymmetric-plan tall building structures. *Engineering Structures*, **33**, 2417-2434, 2011.

[11] T.S. Jan, M.W. Liu, Y.C. Kao, An upper-bound pushover analysis procedure for estimating the seismic demands of high-rise buildings. *Engineering Structures*, **26**, 117-128, 2004.

[12] G. Searer, Poorly worded, ill-conceived, and unnecessary code provisions. *The structural Design of Tall and Special Buildings*, **15**, 533-546, 2006.

[13] R. Englekirk, The impact of prescriptive provisions on the design of high-rise buildings. *The Structural Design of Tall and Special Buildings*, **14**, 455-464, 2005.

[14] J. Moehle, Y. Bozorgnia, T. Yang, The tall buildings initiative. In *Proceedings of the 2007 Convention of the Structural Engineers Association of California*, pp. 26-29, 2007.

[15] C.S. Li, S.S.E. Lam, M.Z. Zhang, Y.L. Wong. Shaking table test of a 1:20 scale high-rise building with a transfer plate system. *Journal of Structural Engineering ASCE*, **132**, 1732-1744, 2006.

[16] X.L. Lu, Y. Zou, W.S. Lu, B. Zhao. Shaking table model test on Shanghai world financial center tower. *Earthquake Engineering & Structural Dynamics*, **36**, 439-457, 2007.

[17] Eurocode 8. Design of structures for earthquake resistance – Part 1: General rules, seismic actions and rules for buildings, EN 1998-1-1. Brussels, Belgium, 2005.

[18] T.J. Sullivan, Direct displacement-based seismic design of steel eccentrically braced frame structures. *Bulletin of Earthquake Engineering*, **11**, 2197-2231, 2013.

[19] T.J. Maley, R. Roldán, A. Lago, T.J. Sullivan, *Effects of response spectrum shape on the response of steel frame and frame-wall structures*. IUSS Press, Pavia, Italy, 2012.

[20] R. Nascimbene, G.A. Rassati, K.K. Wijesundara, Numerical simulation of gusset-plate connections with rectangular hollow section shape brace under quasi-static cyclic loading. *Journal of Constructional Steel Research*, **70**, 177-189, 2011.

[21] S. Santagati, D. Bolognini, R. Nascimbene, Strain life analysis at low-cycle fatigue on concentrically braced steel structures with RHS shape braces. *Journal of Earthquake Engineering*, **16**, 107-137, 2012.

[22] E. Brunesi, R. Nascimbene, G.A. Rassati, Response of partially-restrained bolted beam-to-column connections under cyclic loads. *Journal of Constructional Steel Research*, **97**, 24-38, 2014.

[23] E. Brunesi, R. Nascimbene, G.A. Rassati, Evaluation of the response of partially restrained bolted beam-to-column connection subjected to cyclic pseudo-static loads. *Structures Congress 2013*, pp. 2310-21. Pittsburgh, Pennsylvania, May 2-4, 2013.

[24] E. Brunesi, R. Nascimbene, G.A. Rassati, Seismic response of MRFs with partially-restrained bolted beam-to-column connections through FE analyses. *Journal of Constructional Steel Research*, **107**, 37-49, 2015.

[25] E. Brunesi, R. Nascimbene, GA. Rassati, Seismic performance of steel MRF with partially-restrained bolted beam-to-column connections through FE simulations. *Structures Congress 2014*, pp. 2640-51. Boston, Massachusetts, April 3-5, 2014.

[26] E. Brunesi, D. Bolognini, R. Nascimbene, Evaluation of the shear capacity of precast-prestressed hollow core slabs: numerical and experimental comparisons. *Materials and Structures*, 2014; DOI: 10.1617/s11527-014-0250-6.

[27] E. Brunesi, R. Nascimbene, M. Pagani, D. Beilic. Seismic performance of storage steel tanks during the May 2012 Emilia, Italy, earthquakes. *Journal of Performance of Constructed Facilities ASCE*, 2014; DOI: 10.1061/(ASCE)CF.1943-5509.0000628.

[28] G.A. Rassati, R.T. Leon, S. Noè. Component modeling of partially restrained composite joints under cyclic and dynamic loading. *Journal of Structural Engineering ASCE*, **130**, 343-351, 2004.

[29] A. Braconi, W. Salvatore, R. Tremblay, O.S. Bursi. Behaviour and modelling of partial-strength beam-to-column composite joints for seismic applications. *Earthquake Engineering & Structural Dynamics*, **36**, 142-161, 2007.

[30] M. Latour, V. Piluso, G. Rizzano. Cyclic modeling of bolted beam-to-column connections: component approach. *Journal of Earthquake Engineering*, **15**, 537-563, 2011.

[31] K.K. Wijesundara, R. Nascimbene, T.J. Sullivan, Equivalent viscous damping for steel concentrically braced frame structures. *Bulletin of Earthquake Engineering*, **9**, 1535-1558, 2011.

[32] K.K. Wijesundara, R. Nascimbene, G.A. Rassati, Modeling of different bracing configurations in multi-storey concentrically braced frames using a fiber-beam based approach. *Journal of Constructional Steel Research*, **101**, 426-436, 2014.

[33] EN 10025-2. Hot rolled products of structural steels – Part 2: Technical delivery conditions for non-alloy structural steels. Brussels, Belgium, 2004.

[34] UNI EN 14399-1. High strength structural bolting assemblies or preloading – Part 1: General Requirements. Brussels, Belgium, 2005.

[35] OpenSees. Open system for earthquake engineering simulation. Pacific Earthquake Engineering Research Center, University of California, Berkeley, CA.

[36] E. Brunesi, R. Nascimbene, Extreme response of reinforced concrete buildings through fiber force-based finite element analysis. *Engineering Structures*, **69**, 206-215, 2014.

[37] M.J.N. Priestley, D.N. Grant, Viscous damping in seismic design and analysis. *Journal of Earthquake Engineering*, **9**, 229-255, 2005.

[38] M.H. Scott, G.L. Fenves. Krylov subspace accelerated Newton algorithm: application to dynamic progressive collapse simulation of frames. *Journal of Structural Engineering ASCE*, **136**, 473-480, 2010.